J Therm Anal Calorim (2012) 107:561–571
DOI 10.1007/s10973-011-1551-4

Some heterobimetallic oxalate coordination precursors of lanthanum(III) of the type, $M_3[La(C_2O_4)_3(H_2O)_m]_2 \cdot nH_2O$ (M = Mn(II), Co(II), Ni(II) and Cu(II))

An investigation on the solid-state pyrolytic decomposition

Nidhuban Deb

Received: 15 December 2010 / Accepted: 31 March 2011 / Published online: 11 April 2011

Abstract Heterobimetallic oxalato complex precursors, manganese(II)tetraaquatris(oxalato)lanthanate(III)hexahydrate (MnOLa), cobalt(II)pentaaquatris(oxalato)lanthanate (III)trihydrate (CoOLa), nickel(II)pentaaquatris(oxalato) lanthanate(III)hexahydrate (NiOLa) and copper(II)diaaquatris(oxalato)lanthanate(III)monohydrate (CuOLa) of the type, $M_3[La(C_2O_4)_3(H_2O)_m]_2 \cdot nH_2O$ have been synthesized in aqueous medium. The precursors were characterized by elemental analysis, IR, electronic spectral and powder X-ray diffraction studies. The good crystalline nature with monoclinic structures predominates in MnOLa and NiOLa whereas triclinic structures were found in CoOLa and CuOLa. The solid-state thermal behaviour of the precursors was explored using TG, DTG and DTA in air. The MnOLa generated a mixture species consisting mainly of MnO_2, Mn_3O_4, Mn_5O_8, La_2O_3 and $LaMn_7O_{12}$ at 1000 °C through the formation of several intermediate species at 380 and 570 °C. The studies revealed that CoOLa led mainly to $LaCoO_3$ and La_2CoO_4 along with some oxides of both the cobalt and lanthanum at 1000 °C. In case of nickel analogue the mixture species identified at 1000 °C are mainly of La_2NiO_4, La_2O_3, Ni_2O_3 and NiO_2. In case of CuOLa the product at 1000 °C consisted of La_2CuO_4, $La_2Cu_2O_5$ and oxides of copper and lanthanum. The nature of decomposition of the precursors in nitrogen were seen from DSC study and the kinetic parameters i.e., E^*, $\ln k_0$, $\Delta H^{\#}$, $\Delta S^{\#}$ and order of reaction of all the steps were evaluated and discussed.

N. Deb (✉)
Department of Chemistry, North Eastern Regional Institute of Science and Technology (Deemed University), Nirjuli, Itanagar, Arunachal Pradesh 791109, India
e-mail: nidhubandeb@yahoo.com

Keywords Oxalato · IR · X-ray powder diffraction · Thermal decomposition · TG/DTA/DSC

Introduction

The major role of carboxylate ligands in the assembly of metal-organic porous framework is well known. Interaction of oxalate ligands with lanthanide cations started getting importance in various fields such as ceramic precursors [1], selective extractions of rare earth ions [2]. Due to high and variable coordination modes of lanthanide ions and the competitive interactions between lanthanide and transition metal ions for the organic ligands the compounds on heterobimetallic open frameworks is now a days working in an extensive ways [3–5]. A single phase manganese ferrite powder, $MnFe_2O_4$ with a cubic structure at 1100 °C was synthesized [6] from the thermal decomposition reaction of the mixture, $MnC_2O_4 \cdot 2H_2O$–$FeC_2O_4 \cdot 2H_2O$ (1:2 molar ratio) in air. Later on the decomposition of CuC_2O_4–$CdC_2O_4 \cdot 2H_2O$ (1:1 mol ratios) [7] mixture in air was found to be formed CuO–CdO mixture at the end through three well-defined steps. Spectral, thermal and X-ray diffraction (XRD) studies of the compound, indium(III)bis-oxalato diaquathallate(III)hexahydrate, concluded the molecular formula as $In^{3+}[Tl(C_2O_4)_2(H_2O)_2]_3 \cdot 6H_2O$ [8]. The stoichiometry of the decomposition of the synthesized [9] compounds, $Ba_3[Fe(C_2O_4)_3]_2 \cdot 8H_2O$ and $Sr_3[Fe(C_2O_4)_3]_2 \cdot 2H_2O$ was found to be highly complex, involving at least four changes in the oxidation state of iron, and subsequently the same compounds were studied by Mossbauer effect [10]. The malonato compounds of iron with zinc and with nickel, $Zn_3[Fe(CH_2C_2O_4)_3]_2 \cdot 10H_2O$ [11] and $Ni_3[Fe(CH_2C_2O_4)_3]_2 \cdot 7H_2O$ [12] were found to produce fine particles of mixed metal oxides as end product. Nanosized ferrites of the

stoichiometry $MgFe_2O_4$ and $Ca_2Fe_2O_5$ have been obtained as end products from the citrate precursors, $M_3[Fe(C_6H_5O_7)_2]_2{\cdot}xH_2O$ (M = Mg, Ca) [13]. The ferrites of the same stoichiometry $MgFe_2O_4$ and $Ca_2Fe_2O_5$ were also found to be formed as a solid–solid reaction between α-Fe_2O_3 and MO/MCO_3 during the decomposition of succinato precursor, $M_3[Fe(C_4H_4O_4)_3]_2{\cdot}xH_2O$ (M = Mg, Ca) [14]. The compound of iron with trivalent cobalt, $Co_3[Fe(CH_2C_2O_4)_3]{\cdot}3H_2O$ [15] was found to form monodisperse cobalt ferrite nanoparticles at the end. A detail study on porosity of co-precipitated iron (II) and nickel (II) oxalate samples was also investigated [16] after thermolysis at different temperatures. Thermolysis of polynuclear coordination compounds, $(NH_4)_8[Fe_2Cu(C_2O_4)_8]$ and $[Fe_2Cu(C_2O_4)_2(OH)_4]{\cdot}4H_2O$ were also studied [17]. The compound, $Fe[Fe(C_2O_4)_3]{\cdot}4H_2O$ [18] was synthesized and decomposed finally to ferric oxide through the reduction of the inner Fe(III). It was considered worth while to explore the thermal behaviour of carboxylate compounds and therefore studied the complex precursors $M[M(C_2O_4)_3]{\cdot}xH_2O$(where $x = 4$ for M = Cr(III), $x = 2$ for M = Sb(III) and $x = 9$ for M = La(III)) [19], alkali metal-lanthanide–oxalate system of the types $M^1_3[La(C_2O_4)_3]{\cdot}xH_2O$ (M^1 = Li, Na and K) [20, 21] as well as a similar system with the incorporation of transition metal (Cr(III) and Co(III)) [22] instead of alkali metal. The end products of thermal decomposition were mostly found to be mixture of oxides, mixed metal oxides and carbides. As an extension of our study [23–28] on pyrolytic behaviour of bimetallic carboxylate complexes the more detailed investigation on the system of first raw transition metal–La–$C_2O_4^{2-}$ with respect to thermal behaviour is felt necessary. Therefore, in continuation of our recent study [29] on solid-state pyrolytic fragmentation of $(UO_2^{II})_3[La^{III}(C_2O_4)_3(H_2O)_2]_2{\cdot}8H_2O$ and $Co^{II}(UO_2^{II})_2[La^{III}(C_2O_4)_3(H_2O)_5]_2{\cdot}8H_2O$ and to get a deeper insight on decomposition behaviour of heterobimetallic oxalate complexes this article describes the synthesis, characterization and the thermal decomposition behaviour of four hitherto unknown oxalate complexes of the type, $M_3[La(C_2O_4)_3\ (H_2O)_m]_2{\cdot}nH_2O$ (where M = Mn(II), Co(II), Ni(II) and Cu(II)).

Experimental

Preparation of the complexes

The complex precursors were synthesized by a method similar to the methods adopted [23, 29] earlier. The reagents used were AR grade. Lanthanum nitrate was converted to chloride by digesting repeatedly with concentrated hydrochloric acid. The chloride free lanthanum hydroxide was then prepared by adding sodium hydroxide to lanthanum chloride followed by washing several times with bidistilled water. The lanthanum hydroxide was then dissolved in glacial acetic acid and heated on a steam bath. Adding manganese chloride slowly followed by drop wise addition of saturated solution of oxalic acid separated a light pink precipitate of manganese lanthanum oxalate compound. The precipitate was then filtered, thoroughly washed with deionized water. The light pink compound was dried in air and stored in a desiccator over calcium chloride. Similarly after adding chlorides of cobalt, nickel and copper to the heated solution of acetic acid the corresponding pink, light blue and blue compounds were obtained separately on subsequent addition of saturated solution of oxalic acid. The compounds were dried well and kept in a desiccator. The water contents of the compounds were determined from microanalysis, gravimetrically [18] and thermogravimetrically. The metal contents in the compounds were estimated [30] by known methods; lanthanum was estimated gravimetrically as oxide after double precipitation of it oxalate, manganese as ammonium manganese phosphate, cobalt as $CoSO_4$ after precipitating with α-nitroso β-naphthol and nickel as bis(dimethylglyoximato)nickel(II). The copper content was estimated iodometrically.

Instrumentation

The elemental analysis, IR and diffuse reflectance spectra, thermal data (DTA, TG and DTG in air and DSC in nitrogen) and pyrolysis work (muffle furnace) were done as described earlier [23, 29]. The TG and DTG scanning of all the precursors were done up to 1000 °C, whereas DTA run of the respective manganese, cobalt, nickel and copper analogue were carried out up to 1000, 700, 600 and 700 °C. The temperatures for pyrolysis were chosen from the stable range of thermogram of TG profile. Sometimes the temperature arrest technique was adopted in TG scan to isolate the intermediate species required for the study. In DSC the sample mass taken for the respective precursors were 6.78, 9.69, 9.47 and 8.25 mg. The respective residual mass of the samples taken after the end of the scanning was 4.04, 3.70, 3.75 and 4.19 mg. The powder XRD patterns of the precursors, intermediates and end products were recorded like earlier [23, 25]. The XRD of some of the intermediates and end products were also recorded using Bruker D8 ADVANCE diffractometer.

Results and discussion

The complexes are insoluble in water and common organic solvents, but decompose in strong acid or alkali. Based on the microanalysis, gravimetric and thermogravimetric results the molecular formula of the respective precursors

were concluded as shown in the text. Analysis as calculated for $Mn_3[La(C_2O_4)_3(H_2O)_4]_2{\cdot}6H_2O$: Mn, 13.47%; La, 22.71%; C, 11.79%; H, 2.31% and H_2O, 20.62%; found: Mn, 14.10%; La, 21.22%; C, 11.24%; H, 2.42% and H_2O, 21.00%. Analysis as calculated for $Co_3[La(C_2O_4)_3(H_2O)_5]_2{\cdot}3H_2O$: Co, 14.52%; La; 22.82%; C, 11.84%; H, 2.15% and H_2O, 19.24%; found Co, 14.12%; La, 21.34% C, 12.20%; H, 2.32% and H_2O, 19.00%. Analysis as calculated for $Ni_3[La(C_2O_4)_3(H_2O)_5]_2{\cdot}6H_2O$: Ni, 13.86%; La, 21.87%; C, 11.35%; H, 2.54% and H_2O, 22.69%; found Ni, 14.00%; La, 20.54%; C, 11.76%; H, 2.62% and H_2O, 22.23%. Analysis as calculated for $Cu_3[La(C_2O_4)_3(H_2O)]_2{\cdot}H_2O$: Cu, 18.15%; La, 26.44%; C, 13.72%; H, 0.58% and H_2O, 5.14%; found Cu, 17.86%; La, 25.53%; C, 13.21%; H, 0.74% and H_2O, 5.43%. The IR peaks of the precursors are included in Table 1. The assignments were done similar to earlier studies [22, 23, 29, 31]. The assignments of the different bands for various normal modes of vibration of $C_2O_4^{2-}$ groups are indicative of the proper chelation of ligands and coordinated water to the metal ions. The electronic spectrum of the solid precursor of MnOLa which is a high-spin Mn(II) species absorbs at 20,000 and 27,240 cm^{-1} which are due to spin-allowed and/or *d–d* transition; whereas at 40,980 and 46,720 cm^{-1} are due to respective ligands to metal (or metal to ligands) charge transfer and $\pi \rightarrow \pi^*$ transition. The spectrum of solid sample of CoOLa was compatible with Co(II) species. It displayed a complex multicomponent band centred on 20,000 cm^{-1} (16,890, 18,720, 22,220, 32,250 and 45,450 cm^{-1}). The complexity could be due to either (i) a weak two-electron transition, $4T_{1g}$ (F) $\rightarrow$ $4T_{2g}$ or (ii) mixing of a spin-forbidden band with spin-allowed transitions. Due to complexity of the spectrum in the distorted environment $4A_2 \rightarrow 4T_1$ (P) for tetrahedral and $4T_{1g}$ (F) $\rightarrow$ $4T_{1g}$ (P) for octahedral geometries can be invoked [29, 32, 33] at around 20,000 cm^{-1} along with other nearby transitions. The bands at 32,250 and 45,450 cm^{-1} in the UV region are due to M $\rightarrow$ L or L $\rightarrow$ M charge transfer and intraligand $\pi \rightarrow \pi^*$ transition, respectively. The bands at 20,000 and 27,390 cm^{-1} for NiOLa is due to respective spin-allowed transitions, $3A_{2g} \rightarrow 3T_{1g}$ (F) and $3A_{2g} \rightarrow 3T_{1g}$ (P) which indicates it to be octahedral nickel(II) environment. The $\pi \rightarrow \pi^*$ transition is observed at 45,450 cm^{-1}. The solid sample of copper analogue showed the band at 20,000 and 31,940 cm^{-1} are for *d–d* transition and M $\rightarrow$ L or L $\rightarrow$ M charge transfer, respectively. The band at UV region, 45,450 cm^{-1} is accounted for $\pi \rightarrow \pi^*$ transition. The slight shifting of band position for all the precursor complexes is suggestive of the distortion of ideal geometry for octahedral/tetrahedral or square planar for metal ion(II) environment with likely octahedral geometry for La(III) ions. The powder XRD patterns (Figs. 1, 2, 3 and 4) suggested all the precursors are good crystalline in nature. The precursor, MnOLa (Fig. 1) exhibits strong reflections at $2\theta = 13.30°$ (101), 17.65° (200), 18.25° (102) and crystallize in monoclinic structure with unit cells of dimensions, $a = 13.8662$ Å, $b = 5.2616$ Å, $c = 22.2352$ Å, $\beta = 133.551°$ and $V = 1175.74$ $Å^3$. The precursor, CoOLa (Fig. 2) shows intense reflections at 13.20° (010), 16.70° (100) and 18.65° (−110) and are indexed as a triclinic structure. The unit cell parameters are found to be, $a = 5.4802$ Å, $b = 7.0481$ Å, $c = 4.1284$ Å, $\alpha = 101.328°$, $\beta = 93.544°$, $\gamma = 102.925°$ and $V = 151.45$ $Å^3$. The strong reflections at 13.10° (101), 18.60° (110), 32.80° (102) exhibit by the precursor NiOLa (Fig. 3) and are indexed as a monoclinic structure. The unit cell parameters are found to be, $a = 13.1312$ Å, $b = 5.1223$ Å, $c = 8.2751$ Å, $\beta = 94.271°$ and $V = 555.05$ $Å^3$. The precursor, CuOLa (Fig. 4) shows most intense reflections at 22.75° (010), 36.00° (100), 38.75° (−110) and data were indexed on triclinic unit cell. The unit

Table 1 Selected bands in the IR spectra of $Mn_3[La(C_2O_4)_3(H_2O)_4]_2{\cdot}6H_2O$ (MnOLa), $Co_3[La(C_2O_4)_3(H_2O)_5]_2{\cdot}3H_2O$ (CoOLa), $Ni_3[La(C_2O_4)_3(H_2O)_5]_2{\cdot}6H_2O$ (NiOLa) and $Cu_3[La(C_2O_4)_3(H_2O)]_2{\cdot}H_2O$ (CuOLa)

MnOLa	CoOLa	NiOLa	CuOLa	Band assignments
2800–3840 Sb	2920–3840 Sb	2960–3760 Sb	3000–3720 Sb	ν_{sy} (O–H) + ν_{asy} (O–H) or hydrogen bonding
1640 S	1650 S	1640 S	1660 S	δ_{sy} (H–O–H)
1440–1880 Sb	1430–1820 Sb	1500–1810 Sb	1480–1780 Sb	ν_{asy} (C=O)
1360 m	1360 m	1360 mS	1360 mS	$\nu_{s\ y}$(C–O) and/or ν (C–C)
1320 mS	1320 mS	1320 mS	1320 mS	ν_{sy} (C–O) and/or δ (O–C=O)
800 ms	820 m	830 s, 800 s	820	S ν (M–O) and/or δ (O–C=O) or co-ordinated water
620 s	610 ms	620 m	610 s	Crystal water
520 s	–	–	–	ν (M–O) and/or ν (C–C)
460 mS	460 mS	455 mS	470 S	δ (O–C=O) or ν (M–O) and/or ring deformation
360 s	–	–	360 S	δ (O–C=O) and/or ν (C–C)
290 s	300 ms, 240 s	320 ms, 270 vs	300 mS	π (out-of-plane bending)

b broad; *S* strong; *s* small; *vs* very small and *m* medium

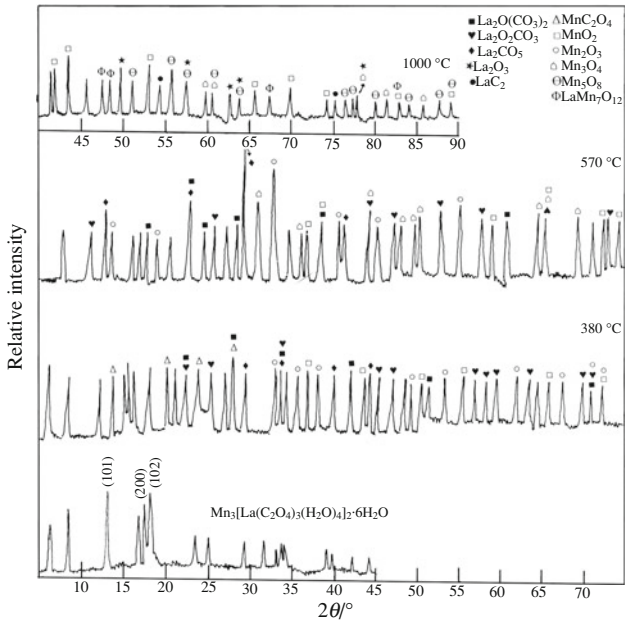

Fig. 1 Prominent peaks in the powder XRD pattern of the complex, $Mn_3[La(C_2O_4)_3(H_2O)_4]_2{\cdot}6H_2O$ (MnOLa) and its pyrolysed products at 380, 570 and 1000 °C

cell parameters are found to be, $a = 2.5473$ Å, $b = 4.3503$ Å, $c = 4.6896$ Å, $\alpha = 113.518°$, $\beta = 91.898°$, $\gamma = 99.772°$ and $V = 46.67$ Å^3.

The TG, DTG and DTA profiles for the thermal decomposition of the precursor, manganese(II)tetraaquatris(oxalato)lanthanate(III)hexahydrate, $Mn_3[La(C_2O_4)_3(H_2O)_4]_2{\cdot}6H_2O$ (MnOLa) in air are shown in Fig. 5. The dehydration starts from 35 °C and continued up to 190 °C in TG. The break at 88 °C is for the removal of two molecules of water and at 136 °C indicates the removal of all water of crystallization. The mass loss of 21% (calcd. 20.62%) at 190 °C is attributed to the formation of anhydrous species through the release of remaining coordinated water molecules. The DTG change between 90 and 210 °C and an endothermic peak in DTA in the range 98–188 °C ($\Delta T_{min} = 150$ °C) with a small shoulder peak at 134 °C corresponds to the dehydration step. The anhydrous species is not stable in TG, rather losses mass of 2.5% slowly in the long temperature range up to 310 °C. This indicates the partial rupture of coordination framework with the breaking of $C_2O_4^{2-}$ moiety, which in turn separates the manganese and lanthanum with their oxalate environment. The product may be the mixture of $3MnC_2O_4$ and $La_2(C_2O_4)_{2.5}$ (found 23.5%; calcd. 24.22%). Both the oxalates undergoes a strong exothermic decomposition in accordance with an exothermic peak in DTA between 263 and 330 °C ($\Delta T_{max} = 300$ °C). The mass loss at the end of this intermediate degradation is 37% corresponding to the TG slope between 310 and 352 °C and DTG change in the range of 310–370 °C. The mass loss apparently may be due to the generation of a mixture species $4MnO_2$ and $La_2O(CO_3)_2$ (calcd. 37.72%) or $2Mn_2O_3$ and $La_2O(CO_3)_2$ (calcd. 40.34%). The species is stable up to 432 °C in TG. The black product isolated at 380 °C gave the effervescence with HCl which indicates the existence of carbonate. The IR bands of the species at 1360–1540, 1020, 840 and 670 cm^{-1} justified about the carbonate group [21, 23] and at 615, 490, 400 and 330 cm^{-1} [24, 34, 35] gave credence to the presence of manganese oxide. The powder XRD (Fig. 1) patterns of the black residue clearly showed reflections corresponding to $La_2O(CO_3)_2$ (JCPDS file no.

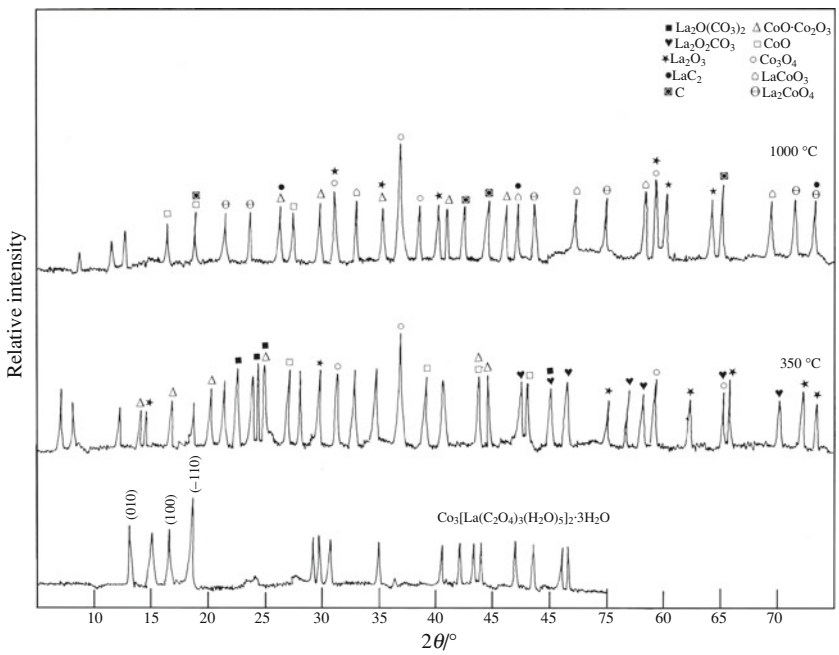

Fig. 2 Prominent peaks in the powder XRD pattern of the complex, $Co_3[La(C_2O_4)_3(H_2O)_5]_2{\cdot}3H_2O$ (CoOLa) and its pyrolysed products at 350 and 1000 °C

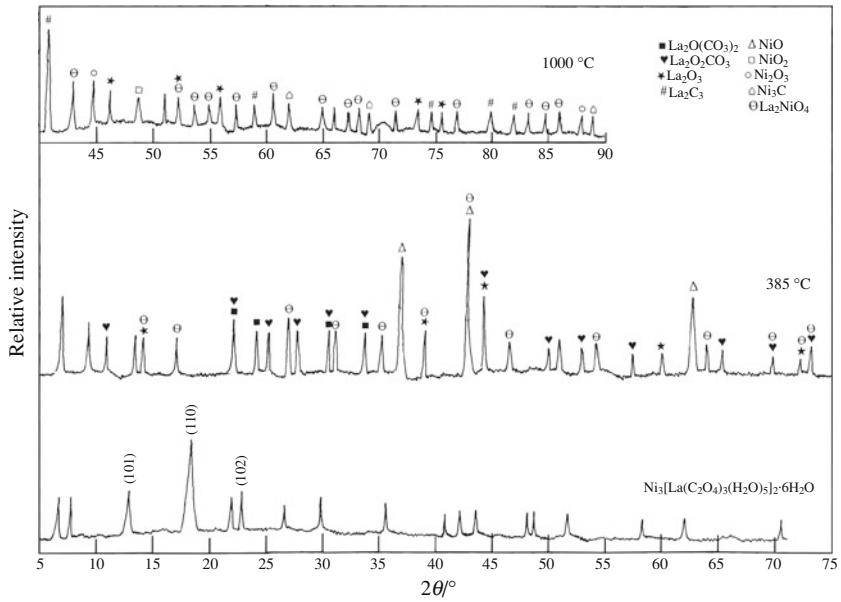

Fig. 3 Prominent peaks in the powder XRD pattern of the complex, $Ni_3[La(C_2O_4)_3(H_2O)_5]_2{\cdot}6H_2O$ (NiOLa) and its pyrolysed products at 385 and 1000 °C

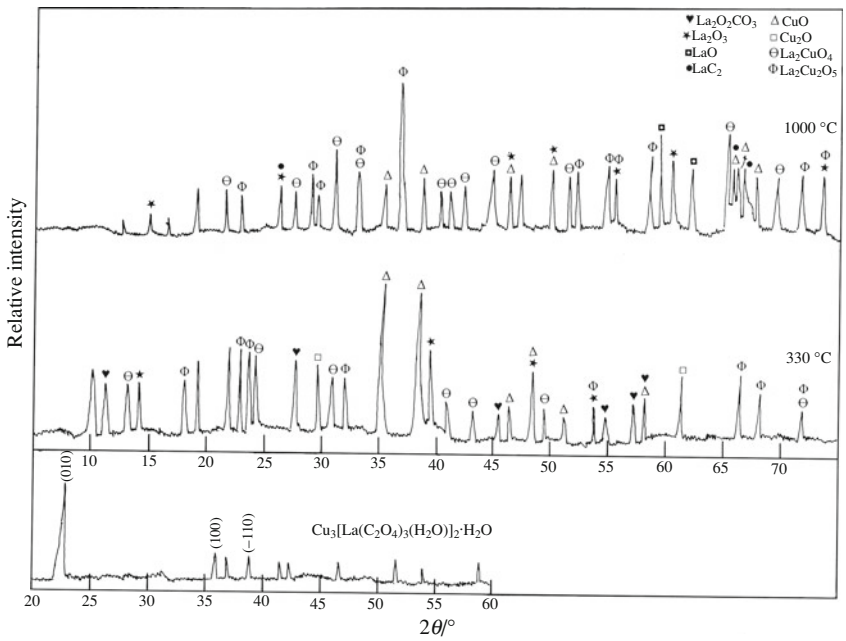

Fig. 4 Prominent peaks in the powder XRD pattern of the complex, $Cu_3[La(C_2O_4)_3(H_2O)]_2{\cdot}H_2O$ (CuOLa) and its pyrolysed products at 330 and 1000 °C

41-0672), $La_2O_2CO_3$ (84-1963) and La_2CO_5 (25-0423) as major phase. The presence of the oxides of manganese, MnO_2 (82-2169) and Mn_2O_3 (76-0150) are also confirmed. A trace of MnC_2O_4 (01-0160) left undecomposed to its oxides as diffraction peaks of it are found in XRD as well as IR bands at 1315 and 815 cm^{-1}. Two strong peaks at 2θ of 15.45° and 48.7° along with other few could not be identified. The simple oxalate of manganese decomposes at 150 [36] and 290 °C [37]. Although in our study manganese oxalate [35] was found to decompose between 246 and 314 °C in air and between 230 and 296 °C in oxygen, here the existence of a part of MnC_2O_4 at calcined temperature at 380 °C in the presence of the oxides of manganese is contemplated in this convoluted process of decomposition. Further, the initial steep and gradually inclined slope in TG between 432 and 547 °C (mass loss 51%) is owing to the decomposition of left part of manganese oxalate and oxycarbonate/dioxycarbonate of lanthanum, respectively. The step may also consist of changes of oxides of manganese from one oxidation state to other. The decomposition temperature [36] of MnO_2 and Mn_2O_3 are 530 and 940 °C, respectively. The exothermic peak between 395 and 515 °C (ΔT_{max} = 403 °C) with two small shoulder peaks at 440 and 482 °C in DTA and a DTG

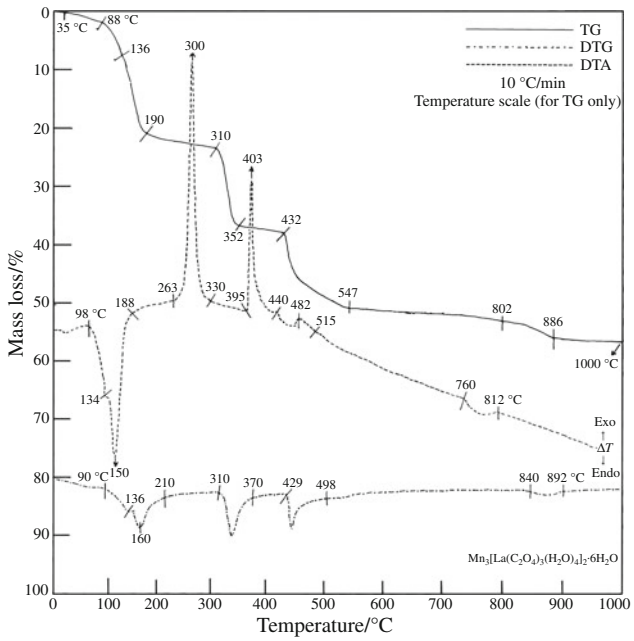

Fig. 5 TG, DTG and DTA profiles of $Mn_3[La(C_2O_4)_3(H_2O)_4]_2{\cdot}6H_2O$ (MnOLa) in air at 10 °C min^{-1}

change (429–498 °C) are accounted for the second decomposition step. The shoulder peaks may be for the interaction and reduction and/or oxidation of the constituent products. These may also be due to the possible phase transformation in the crystal. The species generated at 547 °C was almost stable up to 802 °C with only 2% mass loss. The black powder product isolated at 570 °C showed the XRD (Fig. 1) peaks for $La_2O(CO_3)_2$ (32-0490), $La_2O_2(CO_3)$ and La_2CO_5. The identification of both oxy and dioxycarbonate of lanthanum shows the step in TG between 432 and 547 °C is mainly due to the complete decomposition of manganese oxalate and some part of oxy and dioxycarbonate of lanthanum to La_2CO_5. The presence of all the three oxides of manganese MnO_2, Mn_2O_3 and Mn_3O_4 (80-0382) were also confirmed from XRD data. The IR spectrum did not give the bands for $C_2O_4^{2-}$ group but the bands observed at 600 and 475 cm^{-1} are attributed for Mn_3O_4 [34] along with some other for carbonate groups. No any oxides of lanthanum and mixed metal oxides are identified in the mixture product at 570 °C. The 2% mass loss between 547 and 802 °C which is followed by another slope up to 886 °C (mass loss 56%) is indicative of the decomposition of left amount of oxy and dioxycarbonate of lanthanum. The mass loss apparently indicates the formation of 3MnO and La_2O_3 (calcd. 55.96%) which was stable in TG up to the end of the scanning. The small endotherm in DTA (760–812 °C) and a change in DTG (840–892 °C) correspond to the final moderate decomposition in TG. The pyrolysed species at 1000 °C in furnace as well as the species isolated from the sample pan at the end of TG scan was brown black in colour. The XRD of the powder species shows multiple diffraction lines and confirmed the presence of MnO_2, Mn_3O_4 (brown black) and Mn_5O_8 (72-1427). The La_2O_3 and LaC_2 (82-0629) are also confirmed as other stable constituents in the mixture product. The mixed metal oxide $LaMn_7O_{12}$ (27-0216) are also identified in the end product. A few unidentified peaks may be due to the slight contamination with other species. IR bands of the product corroborated the reality of the oxides. In DSC study in nitrogen (Table 2) all the steps are found to be first order. The first endothermic peak between 90.9 and 182.4 °C is for the dehydration and is similar to that in air. The subsequent peaks in DSC are not in accordance with the peaks in DTA in air. Therefore, the decomposition behaviour does not comply with air. The second endothermic peak in the range 362.7–442.1 °C manifests to the decomposition of the anhydrous species. The high activation energy (E^*) (Table 2) for the step indicative [38] of the slow fragmentation of anhydrous species. The species generated immediately undergoes further changes by an intricate process of interaction and/or decomposition which is supported by the display of overlapping endotherm and exotherm in the range of 443.9–590.4 °C. The interaction may be the type of reduction of the possible intermediate oxides by the evolve CO (g), disproportionation of CO (g) to CO_2 (g) and C, gas–solid and solid–solid reaction of the intermediates [27, 28]. The enlarged endotherm demarcated between 443.9 and 550.2 °C is corroborated to the generation of some species through the interaction of the constituents in the mixture which are unstable in the process, and immediately decomposed to stable products supported by small exotherm between 502.9 and 590.4 °C. Further changes occurred in the decomposed species as evidenced by another small exothermic peak in the range 601.3–669.1 °C. The process of leading the end product may be slow as evidence by high E^* of the path. The mass loss of 40.41% of the annealed sample up to 670 °C led a black product. The negative ΔS value of the stages indicative of the respective reactions steps are slower than normal [39] and the species are more ordered in the activated state than the reactants for that steps.

The thermal profiles (TG, DTG and DTA) of cobalt(II)pentaaquatris(oxalato)lanthanate(III)trihydrate, $Co_3[La(C_2O_4)_3(H_2O)_5]_2{\cdot}3H_2O$ (CoOLa) are shown in Fig. 6. The slope in TG curve with break at 90 and 133 °C indicates the removal of first and second molecule of crystal water. The inclined slope between 170 and 233 °C (mass loss, found, 19%; calcd., 19.24%) indicates the complete elimination of the remaining molecules of coordinated water. The small endothermic peak at 112 °C and a large endothermic peak in DTA in the range 165–250 °C ($\Delta T_{min} = 215$ °C) and a DTG

Table 2 DSC data of $Mn_3[La(C_2O_4)_3(H_2O)_4]_2{\cdot}6H_2O$ (MnOLa), $Co_3[La(C_2O_4)_3(H_2O)_5]_2{\cdot}3H_2O$ (CoOLa), $Ni_3[La(C_2O_4)_3(H_2O)_5]_2{\cdot}6H_2O$ (NiOLa) and $Cu_3[La(C_2O_4)_3\ (H_2O)]_2{\cdot}H_2O$ (CuOLa) in nitrogen at 10 °C min^{-1}

Compound	Step	Temperature range/°C	Peak temperature/°C	ln k_0/s^{-1}	E^*/kJ mol^{-1}	ΔH/kJ mol^{-1}	ΔS/JK^{-1} mol^{-1}	Order of reaction	Reaction
MnOLa	a	90.9–182.4 (endo.)	147.9	30.05 ± 0.64	120.21 ± 2.59	609.23	1447.46	1.15 ± 0.02	Dehydration
	b	362.7–442.1 (endo.)	415.0	54.85 ± 1.18	338.46 ± 7.31	246.19	357.84	1.05 ± 0.02	Decomposition
	c	443.9–550.2 (endo. flat)	497.3	36.15 ± 0.78	264.57 ± 5.71	102.67	133.28	1.09 ± 0.02	Decomposition
	d	502.9–590.4 (exo. flat)	554.3	21.06 ± 0.45	187.14 ± 4.04	−291.22	−349.35	0.97 ± 0.02	Decomposition
	e	601.3–669.1 (exo.)	646.4	60.26 ± 1.30	494.42 ± 10.68	−374.09	−406.79	0.91 ± 0.01	Decomposition
CoOLa	a	90.1–141.3 (endo. flat)	117.1	46.25 ± 0.99	163.94 ± 3.54	19.60	50.25	1.15 ± 0.02	Dehydration
	b	160.6–245.2 (endo.)	220.5	39.03 ± 0.84	175.33 ± 3.78	580.08	1175.53	1.14 ± 0.02	Dehydration and decomposition
	c	352.1–418.9 (endo.)	392.8	69.28 ± 1.49	407.32 ± 8.79	364.02	546.71	1.10 ± 0.02	Decomposition
NiOLa	a	103.0–167.9 (endo. flat)	123.8	29.20 ± 0.63	113.75 ± 2.45	29.84	75.20	1.16 ± 0.02	Dehydration
	b	202.3–290.9 (endo.)	257.8	39.37 ± 0.85	191.92 ± 4.14	497.71	937.67	1.17 ± 0.02	Dehydration and decomposition
	c	327.3–401.7 (endo.)	373.8	57.86 ± 1.25	332.12 ± 7.17	331.17	512.01	1.18 ± 0.02	Decomposition
	c_1	341.2–363.2 (endo. sh)	352.5	161.90 ± 3.49	861.23 ± 18.6	11.22	17.93	1.05 ± 0.02	Decomposition
CuOLa	a	283.4–324.9 (exo.)	292.9	101.49 ± 2.19	498.92 ± 10.78	−158.40	−279.89	1.53 ± 0.03	Dehydration and decomposition
	b	652.6–661.2 (endo.)	656.0	465.21 ± 10.05	3615.82 ± 78.12	0.90	0.97	0.98 ± 0.02	Reduction

change between 160 and 260 °C are for the dehydration step. The anhydrous form generated undergone the partial rupture of oxalate ligands up to 314 °C with only 2% mass loss. This may be due to the split of linkage of cobalt and lanthanum with the separation of $3CoC_2O_4$ and $La_2(C_2O_4)_{2.7}$ (mass loss, found, 21%; calcd. 21.41%). Similar partial breaking of chelating $C_2O_4^{2-}$ and $C_4H_4O_6^{2-}$ groups in the process of decomposition of other lanthanate precursors are also observed earlier [19, 22, 23, 38]. The mixture of both in the prevailing condition was not stable. These undergo vigorous decomposition to their respective products in accordance with a steep slope in TG between 314 and 335 °C. A strong exothermic peak in DTA in the range of 300–360 °C (ΔT_{max} = 320 °C) with a small shoulder peak at 340 °C and DTG change between 310 and 360 °C are accounted for this major decomposition. The species generated at 335 °C in TG apparently indicates it to be a mixture of Co_3O_4 and La_2O_3 (calcd. 53.44%) or 3CoO and La_2O_3 (calcd. 54.75%) against the observed mass loss of 53%. The species was almost stable up to 423 °C and afterwards losses weight very slowly in long temperature range up to 950 °C. Considering the stability of the product generated at 335 °C we isolated the pyrolysed product at 350 °C in furnace as well as from TG run. The black species isolated was subjected to powder XRD and IR study. The pattern of peaks displayed in XRD confirmed the species is mainly a mixture of $CoO{\cdot}Co_2O_3$ (02-1079), La_2O_3 (74-1144), CoO (01-1227) and Co_3O_4 (76-1802). The presence of the few peaks for $La_2O(CO_3)_2$ and $La_2O_2CO_3$ suggests the decomposition takes place through the oxy and dioxycarbonate formation. The major part of these immediately decomposes to oxide and the left part remain undecomposed herein major decomposition process. The undecomposed part remains stable up to 423 °C in TG in the presence of identified oxides of manganese and lanthanum. The presence of some other species cannot be ruled out as some unidentified diffraction peaks recorded in the pattern. The IR bands observed at 655, 640, 560, 415 and

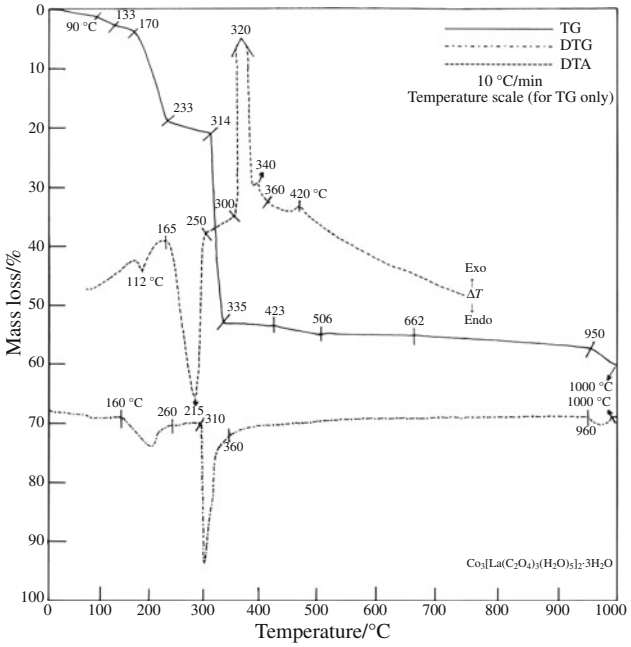

Fig. 6 TG, DTG and DTA profiles of $Co_3[La(C_2O_4)_3(H_2O)_5]_2{\cdot}3H_2O$ (CoOLa) in air at 10 °C min^{-1}

350 cm^{-1} for the oxides and at 1350–1540, 1025, 845 and 715 cm^{-1} for CO_3^{2-} of the oxy and dioxycarbonate [21] further authenticated their presence. Further, both the oxy and dioxycarbonate decomposes slowly which is supported by a slender TG slope between 423 and 506 °C and a small exotherm at 420 °C in DTA. The slow weight loss in TG also may be due to the immediate reduction of a part of Co_3O_4 to CoO by CO (g) evolved during decomposition of carbonate group. Moreover, the mass loss may be accounted due to oxidation of another part of Co_3O_4 to Co_2O_3 which led to form more $CoO{\cdot}Co_2O_3$. The mixture species of the oxides are stable in TG up to 662 °C and subsequently very slow mass loss occurred until 950 °C with 57.5%. Further at the end, another slope between 950 and 1000 °C with 60% mass loss is indicative of the development of new phases through solid–solid reaction of the oxide species of both the metals. The DTG change between 960 and 1000 °C corresponds for this changeover. The DTA curve up to 700 °C has not shown any peaks afterwards of 420 °C. The mass loss apparently indicates it is the mixture of Co_2O_3 and La_2O_3 or their mixed oxide of the type $2LaCoO_3$ (calcd. 59.59%). The XRD of the black residue isolated from the sample pan at the end of the TG scan as well as after pyrolysis at the furnace at ~1000 °C confirmed the presence of $LaCoO_3$ (48-0123) and La_2CoO_4 (72-0937). The presence of $CoO{\cdot}Co_2O_3$, Co_3O_4 and La_2O_3 in the end product is also confirmed. This indicates a part of oxides undergone solid–solid reaction forming double oxides and the remaining part left as independent products in the mixture species. The appearance of few diffraction lines for CoO (01-1227) also proved its presence till end; a major part of which produced at 350 °C may be used for mixed metal oxide formation and remaining unreacted till the end. A few peaks for LaC_2 (82-0629) and C (79-1473) are also identified in the product. The presence of the oxides is also verified from IR bands. The mass loss step at the end of TG may be due to conversion of a part of La_2O_3 to carbides at high temperature as well as plausible oxidation and/or reduction event while forming double oxides. In DSC study (Table 2) the first flat endothermic peak between 90.1 and 141.3 °C is for the removal of one or two molecules of water. This is followed by display of another endotherm in the range 160.6–245.2 °C. This corresponds to the elimination of residual water molecules accompanied by the partial decomposition of the deaquated compound. Subsequent large endotherm between 352.1 and 418.9 °C may be accounted for the further decomposition of the partially decomposed species. The decomposed product is stable in the profile up to the end of the scanning. The black residue isolated at the end of the scanning up to 670 °C (mass loss, 61.8%) indicates the species may be a mixture of oxides of both cobalt and lanthanum along with a trace of mixed metal oxide and carbon. All the steps are found to be first order kinetics and mostly the values of ΔH and ΔS are found to be dependent on the area of the endotherm of the respective changes. The higher value of E^* for the final step as compared to the dehydration steps manifest it to be a process of slow decomposition with the possible existence of reduction and interaction phenomena in inert atmosphere.

The thermal profiles (TG, DTG and DTA) of nickel(II) pentaaquatris(oxalato)lanthanate(III)hexahydrate, $Ni_3[La(C_2O_4)_3(H_2O)_5]_2{\cdot}6H_2O$ (NiOLa) are shown in Fig. 7. The mass loss started in TG from 40 °C and an inclined slope up to 200 °C is for the departure of six molecules of water of crystallization (mass loss, observed 8.5%, calcd. 8.5%). A break at 140 °C (mass loss, observed 6%, calcd. 5.67%) is for the release of four molecules of water. Further, another distinct slope up to 282 °C is for the release of all coordinated water with an indication for the formation of anhydrous compound (mass loss, observed, 23%, calcd. 22.69%). The DTG change between 210 and 310 °C and a small endotherm at 123 °C and another large endothermic peak in DTA in the range 200–283 °C ($\Delta T_{min} = 257$ °C) accounts for these dehydration steps. The display of subsequent inclined slope between 282 and 337 °C (observed mass loss, 26%) gives the credence [20, 21, 23] of the release of $3NiC_2O_4$ and $La_2(C_2O_4)_{2.5}$ (calcd. 26.15%). Both the oxalates decompose corresponding to a steep slope from 337 to 370 °C. The 57.5% mass loss at 370 °C may

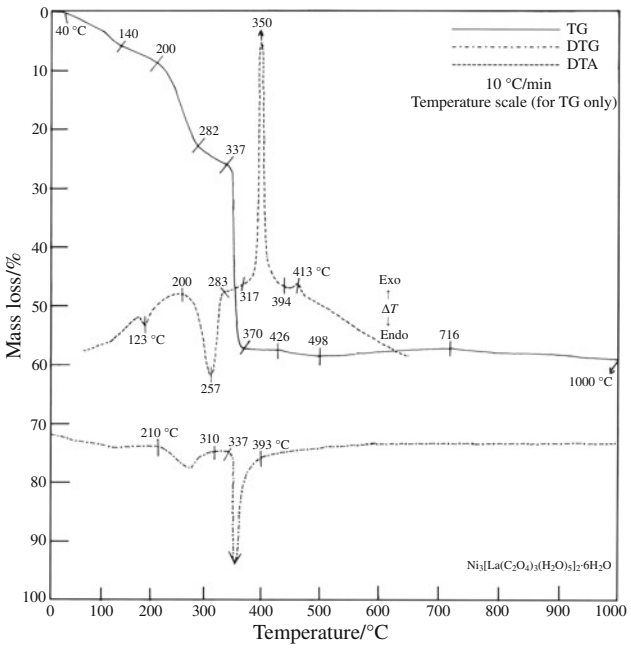

Fig. 7 TG, DTG and DTA profiles of $Ni_3[La(C_2O_4)_3(H_2O)_5]_2{\cdot}6H_2O$ (NiOLa) in air at 10 °C min^{-1}

be for the existence of the mixture [3NiO + La_2O_3] (calcd. 56.7%) or [3NiO + 2LaO] (calcd. 57.96%) and is stable in TG up to 426 °C. The DTG between 337 and 393 °C and an exothermic peak in DTA in the range 317–394 °C (ΔT_{max} = 350 °C) are accounted for instantaneous decomposition of the oxalates of both the metal. Considering the stability, the species was isolated by temperature arrest technique at 385 °C. The black pyrolysed product of the precursor heated up to 385 °C in muffle furnace was also collected. The IR bands at 650, 460 and 415 cm^{-1} indicates the presence of oxides of metals along with the observed bands for CO_3^{2-}. The powder XRD (Fig. 3) of the product shows multiple diffraction peaks and confirmed that the species is composed of $La_2O(CO_3)_2$ (41-0672), $La_2O_2CO_3$ (84-1963) and La_2O_3 (74-1144). This indicates that the partially fragmented oxalates of lanthanum produced in the mixture at 337 °C decomposes simultaneously to its oxy and dioxycarbonate along with it oxide. The presence of trace of NiO (78-0643) is also confirmed. The existence of several diffraction peaks for La_2NiO_4 (86-1668) confirmed its formation through the solid–solid interaction of a little parts of both the oxides of nickel and lanthanum in the stable range of TG up to 426 °C. The existence of a very small exotherm at 413 °C in DTA gives a faith of the interaction of the solid products. The 1% mass loss shown in TG from 426 to 498 °C and subsequent mass gain of only 1% up to 716 °C may be for release of new products. Afterwards, the stable nature of the TG profile up to 1000 °C suggests about the stability of the end products. The XRD of the isolated product at the end of TG scan as well as products after pyrolysis at 1000 °C in furnace confirmed it mainly to be consisted of La_2NiO_4 and La_2O_3. The presence of Ni_2O_3 (14-0481) and NiO_2 (85-1977) also confirmed which indicates the residual NiO identified at 385 °C completely oxidise to the above oxide products which is substantiated by mass gain in TG and appearance of a small exothermic peak in DTA at 413 °C. A trace of carbides of both the metal, Ni_3C (77-0194) and La_2C_3 (82-0622) are also identified from the XRD. The slight mass gain also may be due to these carbides. The IR bands also confirmed the presence of oxides. The DSC profile (Table 2) displayed three endothermic peaks. The first flat peak between 103 and 167.9 °C may be accounted for the departure of all the molecules of crystal water. The second large endotherm in the range 202.3–290.9 °C corresponds to the disorder of some bridging coordinated $C_2O_4^{2-}$ groups with the simultaneous release of coordinated water. The third endothermic peak between 327.3 and 401.7 °C is due to rapid breakdown of the chelate structure leading to oxide products. The small shoulder peak (341.2–363.2 °C) in the last endotherm with high E^* might be due to slow probable changes of the intermediates released during the main decomposition process. The 60.4% mass loss at the end indicates the complete breakdown of the chelating structure.

The thermal profiles (TG, DTG and DTA) of copper(II)diaaquatris(oxalato)lanthanate(III)monohydrate, $Cu_3[La(C_2O_4)_3(H_2O)]_2{\cdot}H_2O$ (CuOLa) are shown in Fig. 8. The slow mass loss between 40 and 284 °C in TG indicates the loss of two molecules of water. The last molecule of water removes during the decomposition corresponding to a steep

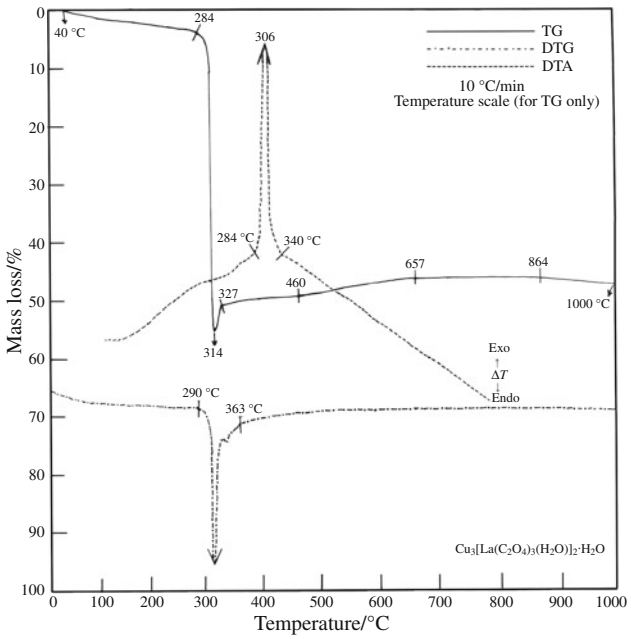

Fig. 8 TG, DTG and DTA profiles of $Cu_3[La(C_2O_4)_3\ (H_2O)]_2{\cdot}H_2O$ (CuOLa) in air at 10 °C min^{-1}

slope in TG (284–314 °C). The mass loss of 55.5% at 314 °C and then a total gain of 9.5% mass up to 657 °C in TG through three distinct steps indicate the phase wise oxidation and reduction of the products produced at 314 °C. The 55.5% mass loss at 314 °C apparently may be due to the formation of [2CuO + 2LaO] (calcd. 55.37%) or [$Cu_2O + La_2O_3$] (calcd. 55.37%). The isolated black product from TG and furnace up to 330 °C subjected to XRD study. The multiple diffraction pattern (Fig. 4) confirmed the presence of $La_2O_2CO_3$, La_2O_3, CuO (80-1916) and Cu_2O (78-2076). The mixed metal oxides, La_2CuO_4 (82-2142) and $La_2Cu_2O_5$ (86-1295) are also confirmed in the product. The IR bands at 640, 615, 500, 420 and 405 cm^{-1} are identified for the oxides and at 1020 and 665 cm^{-1} for CO_3^{2-}. The 4.5% gain of mass from 314 to 327 °C (overall 51% mass loss at 327 °C) may be due to reduction of a part of copper oxide from Cu^{2+} to Cu^{+} through solid–gas interaction by evolved CO (g). The formation of mixed metal oxides through the solid–solid reaction of the major parts of oxides of both the metal occurs between 314 and 327 °C may also be responsible for the mass gain. In the process of heating in TG the identified products further gained mass of 1.5% from 327 to 460 °C and subsequently further 3.5% up to 657 °C. The DTG change between 290 and 363 °C and an exothermic peak in DTA in the range 284–340 °C (ΔT_{max} = 306 °C) corresponds to this oxidative decomposition and reduction processes. The product generated at 657 °C was stable up to 864 °C which further losses mass of 1% till 1000 °C with cumulative mass loss of 47%. The end product obtained from TG and the pyrolysed product in furnace up to 1000 °C was light greenish black in colour and sticky in nature. The XRD confirmed it to be consisted of La_2O_3, CuO, La_2CuO_4 and $La_2Cu_2O_5$. A trace of LaO (33-0716) and LaC_2 (23-1142) are also detected in the product. The IR bands also confirmed the existence of oxides. The DTA curve did not display any further peak up to 700 °C which indicates no major decomposition occurred in the mixture species isolated at 330 °C. In DSC study (Table 2) in nitrogen showed an exothermic peak between 283.4 and 324.9 °C is for the simultaneous dehydration and decomposition of the compound to the oxide products. Further a very small endothermic change noticed between 652.6 and 661.2 °C with a very large E^* value may be due to reduction of the some species in the product. The mass loss at the end of the scanning was found to be 49.21%.

Conclusions

All the precursors are well crystalline in nature with monoclinic structures predominate in MnOLa and NiOLa, whereas triclinic structures prevail in CoOLa and CuOLa. A good chelation of oxalate ligands with both the metal ions are ascertained in all the precursors and these reflects the intricate decomposition pattern of the precursors. The study revealed that the precursors released their coordinated water molecules during the rupture of metal–lanthanum linkages. Several unstable intermediate phases generated during decomposition in air of all the complexes where intermittent oxy and dioxycarbonates of lanthanum are common which ultimately decomposed to oxides. Unlike other precursors, in manganese analogue these carbonates show their stability at higher temperature between 547 and 802 °C in the presence of oxides of manganese and La_2CO_5. The oxidation and reduction phenomena of intermediates during the decomposition were prominent in all the cases. The study revealed that the synthesis of mixed metal oxides, $LaMn_7O_{12}$, $LaCoO_3$, La_2CoO_4, La_2NiO_4, La_2CuO_4 and $La_2Cu_2O_5$ along with oxides and carbides of individual metal are possible through the pyrolysis route of the precursors at the end. The study shown that the mixed metal oxides are generated at lower temperature of 330 and 385 °C in case of copper and nickel analogue whereas release of these are noticed at much higher temperature in manganese and cobalt precursors. All the major decomposition steps in DSC study in nitrogen are endothermic changes except copper analogue where an exothermic change was noticed.

References

1. Kareiva A, Harlan CJ, MacQueen DB, Cook RL, Barron AR. Carboxylate-substituted alumoxanes as processable precursors to transition metal–aluminium and lanthanide–aluminium mixed-metal oxides: atomic scale mixing via a new transmetalation reaction. Chem Mater. 1996;8:2331–40.
2. Ohto K, Yano M, Inoue K, Nagasaki T, Goto M, Nakashio F, Shinkai S. Effect of coexisting alkaline metal ions on the extraction selectivity of lanthanide ions with calixarene carboxylate derivatives. Polyhedron. 1997;16:1655–61.
3. Gu X, Xue D. Selected controlled synthesis of three-dimensional 4d–4f heterometallic coordination frameworks by lanthanide carboxylate subunits and silver centers. Cryst Growth Des. 2006;6:2551–7.
4. Gu X, Xue D. Spontaneously resolved homochiral 3D lanthanide–silver heterometallic coordination framework with extended helical Ln–O–Ag subunits. Inorg Chem. 2006;45:9257–61.
5. Gu X, Xue D. 3D coordination framework [Ln4(μ3-OH) 2Cu615(IN)8(OAc)3](IN = isonicotinate): employing 2D layers of lanthanide wheel clusters and 1D chains of copper halide clusters. Inorg Chem. 2007;46:5349–53.
6. Gabal MA, Ata-Allah SS. Concerning the cation distribution in $MnFe_2O_4$ synthesized through the thermal decomposition of oxalates. J Phys Chem Solids. 2004;65:995–1003.
7. Gabal MA. Non-isothermal kinetics and characterization studies for the decomposition course of CuC_2O_4–CdC_2O_4 mixture in air. J Phys Chem Solids. 2007;68:1610–6.
8. Kebede T, Ramana KV, Prasada Rao MS. Some studies on thallium oxalates XIV Indium(III)bis-oxalatodiaquathallate(III)hexahydrate. Thermochim Acta. 2002;381:31–6.

9. Gallagher PK. Thermal decomposition of barium and strontium trisoxalato ferrate(III). Inorg Chem. 1965;4:965–70.
10. Gallagher PK, Kurkjian CR. A study of the thermal decomposition of some complex oxalates of iron(III) using the Massbauer effect. Inorg Chem. 1966;5:214–9.
11. Randhawa BS, Kaur M. Preparation of zinc ferrite from the thermolysis of zinc tris(malonato)ferrate(III)decahydrate. Indian J Eng Mater Sci. 2003;10:148–50.
12. Randhawa BS, Singh J, Kaur H, Kaur M. Preparation of ferrite from thermolysis of nickel tris(malonato)ferrate(III)heptahydrate precursor. Ceram Int. 2010;36:1993–6.
13. Randhawa BS, Kaur M. Preparation of magnesium and calcium ferrites from the thermolysis of $M_3[Fe(cit)_2]_2{\cdot}xH_2O$ precursors. J Radioanal Nucl Chem. 2004;261:569–76.
14. Randhawa BS, Gandotra K. Preparation of ferrites from the thermal decomposition of manganese and calcium tris(succinato)ferrates(III) precursors. J Therm Anal Calorim. 2007;90: 887–91.
15. Randhawa BS, Gupta M, Kaur M. Preparation of cobalt ferrite from the thermolysis of cobalt tris(malonato)ferrite(III)trihydrate precursor. Ceram Int. 2009;35:3521–4.
16. Hayrapetyan SS, Khachatryan HG. The porosity of partly sintered nickel iron oxalates. Microporous Mesoporous Mater. 2006;89: 33–8.
17. Marinescu G, Patron L, Carp O, Diamandescu L, Stanica N, Meghea A, Brezianu M, Grenier J-C, Etourneau J. Polynuclear coordination compounds as precursors for $CuFe_2O_4$. J Mater Chem. 2002;12:3458–62.
18. Sanyal TK, Dass NN. Synthesis and the thermal decomposition of iron(III)tris(oxalate)ferrate(III)tetrahydrate. J Inorg Nucl Chem. 1980;42:811–3.
19. Deb N, Baruah SD, Sen Sarma N, Dass NN. Synthesis, characterization and thermal investigation of $M[M(C_2O_4)_3]{\cdot}xH_2O$ ($x = 4$ for M = Cr(III); $x = 2$ for M = Sb(III) and $x = 9$ for M = La(III)). Thermochim Acta. 1998;320:53–67.
20. Deb N, Baruah SD, Dass NN. Synthesis, characterization and the thermal decomposition of lithium tris(oxalate)lanthanum(III)nonahydrate and sodium tris(oxalate)lanthanum(III)octahydrate. Thermochim Acta. 1999;326:43–52.
21. Deb N. Synthesis, characterization and the thermal decomposition of potassium tris(oxalate)lanthanum(III)nonahydrate. Thermochim Acta. 1999;338:27–33.
22. Deb N. Thermal investigations of $M[La(C_2O_4)_3]{\cdot}xH_2O$ (M = Cr(III) and Co(III)). J Therm Anal Calorim. 2002;67: 699–712.
23. Deb N. An investigation on the solid-state thermal decomposition of bimetallic oxalate and tartrate coordination precursors of lanthanum(III) and palladium(II) ions. J Anal Appl Pyrol. 2008; 82:223–8.
24. Deb N. Thermal decomposition of manganese(II)bis(oxalato)nickelate(II)tetrahydrate. J Therm Anal Calorim. 2005;81: 61–5.
25. Deb N. Cadmium(II)bis(oxalato)cobaltate(II)pentahydrate: thermal decomposition. J Therm Anal Calorim. 2004;75:837–46.
26. Deb N. Thermal decomposition behaviour of zinc(II)bis(oxalato)cobaltate(II)pentahydrate. Ind J Chem. 2003;42A:506–9.
27. Deb N. An investigation on the solid state pyrolytic decomposition of bimetallic oxalate precursors of Ca, Sr and Ba with cobalt: a mechanistic approach. J Anal Appl Pyrol. 2007;80:389–99.
28. Deb N. A mechanistic approach on the solid state thermal decomposition of bimetallic oxalate coordination compounds of Mn(II), Fe(II) and Cu(II) with cobalt. J Anal Appl Pyrol. 2007; 78:24–31.
29. Deb N. An investigation on the solid-state thermal decomposition behaviour of uranyl(II)diaquatris(oxalato)lanthanate(III)octahydrate and cobalt(II)uranyl(II)pentaquatris(oxalate)lanthanate(III)-octahydrate. J Anal Appl Pyrol. 2010;87:269–75.
30. Basset J, Denny RC, Jeffery GH, Mendhan J. Vogel's text book of quantitative inorganic analysis. 4th ed. Essex: Longman; 1985.
31. Nakamoto K. Infrared spectra of inorganic and co-ordination compounds. 2nd ed. New York: Wiley; 1969. p. 83, 89, 219, 245.
32. Cotton FA, Wilkinson G. Advanced inorganic chemistry. New York: Wiley; 1988. p. 730.
33. Deb N, Gogoi PK, Dass NN. Synthesis and thermal decomposition of cobalt(II)bis(oxalato)cobaltate(II)tetrahydrate. J Therm Anal Calorim. 1989;35:27–34.
34. Bently FF, Smithson LD, Rozek AL. Infrared spectra and characteristic frequencies 300–700 cm^{-1}. New York: Wiley; 1968. p. 103.
35. Deb N, Gogoi PK, Dass NN. Thermal decomposition of manganese(II)bis(oxalato)manganese(II)tetrahydrate. Thermochim Acta. 1989;145:77–86.
36. Dean JA. Lange's handbook of chemistry. New York: McGraw Hill; 1987. p. 4–75.
37. Nagase K, Sato K, Tanaka N. Thermal dehydration and decomposition reactions of bivalent metal oxalates in the solid state. Bull Chem Soc Jpn. 1975;48:439–42.
38. Deb N. Thermal decomposition behaviour of lanthanum(III)tris-tartrato lanthanate(III)decahydrate. J Therm Anal Calorim. 2004;78:227–37.
39. Jisha KR, Suma S, Sudarsanakumar MR. Synthesis, spectral characterisation and thermal studies of zirconyl complexes of biologically active molecules. J Therm Anal Calorim. 2010;99: 509–13.